Molecular Therapy
Methods & Clinical Development
Original Article

Transduction characteristics of alternative adeno-associated virus serotypes in the cat brain by intracisternal delivery

Jacqueline E. Hunter,[1] Caitlyn M. Molony,[2] Jessica H. Bagel,[2] Patricia A. O'Donnell,[2] Stephen G. Kaler,[3,5] and John H. Wolfe[1,2,4]

[1]Research Institute of Children's Hospital of Philadelphia, 502-G Abramson Research Center, 3615 Civic Center Boulevard, Philadelphia, PA 19104, USA; [2]W.F. Goodman Center for Comparative Medical Genetics, School of Veterinary Medicine, University of Pennsylvania, Philadelphia, PA 19104, USA; [3]Section on Translational Neuroscience, Eunice Kennedy Shriver National Institute of Child Health and Human Development, Bethesda, MD 20892, USA; [4]Department of Pediatrics, Perelman School of Medicine, University of Pennsylvania, Philadelphia, PA 19104, USA

Multiple studies have examined the transduction characteristics of different AAV serotypes in the mouse brain, where they can exhibit significantly different patterns of transduction. The pattern of transduction also varies with the route of administration. Much less information exists for the transduction characteristics in large-brained animals. Large animal models have brains that are closer in size and organization to the human brain, such as being gyrencephalic compared to the lissencephalic rodent brains, pathway organization, and certain electrophysiologic properties. Large animal models are used as translational intermediates to develop gene therapies to treat human diseases. Various AAV serotypes and routes of delivery have been used to study the correction of pathology in the brain in lysosomal storage diseases. In this study, we evaluated the ability of selected AAV serotypes to transduce cells in the cat brain when delivered into the cerebrospinal fluid via the *cisterna magna*. We previously showed that AAV1 transduced significantly greater numbers of cells than AAV9 in the cat brain by this route. In the present study, we evaluated serotypes closely related to AAVs 1 and 9 (AAVs 6, AS, hu32) that may mediate more extensive transduction, as well as AAVs 4 and 5, which primarily transduce choroid plexus epithelial (CPE) and ependymal lining cells in the rodent brain. The related serotypes tended to have similar patterns of transduction but were divergent in some specific brain structures.

INTRODUCTION

Lysosomal storage diseases (LSDs) have a single metabolic defect present in multiple cell types throughout the brain, and often in other organs of the body as well. Most of the LSDs are caused by mutations in structural enzyme genes.[1] While the delivery of purified enzyme into the cerebrospinal fluid (CSF) has been moderately successful in both animal models and humans,[2–14] recombinant enzymes have short half-lives and require repeated injections for sustained therapeutic benefit. Gene therapy can address the limitations of enzyme replacement therapy by widespread transduction of brain cells from a single injection for continuous production of the normal gene product. Adeno-associated viruses (AAVs) are particularly beneficial as they transduce both dividing and nondividing cells and have a good safety profile.

Multiple studies have investigated transduction characteristics of AAV serotypes in rodent brains using several different routes of administration[15–25] and others have been conducted in large animal models, including large animal models of LSDs.[26–36] Testing in large animal models is necessary because the transduction patterns observed in the rodent brain do not necessarily translate to large animal models of human diseases. The differences in size and structure of the large animal brain also lead to significant differences in transduction characteristics that need to be considered when developing therapies for the human brain.[1,37] For example, AAV-PHP.B was selected for high transduction in the mouse brain and produced equal CNS transduction in mice regardless of injection route (intravascular, intracisternal, or intraventricular).[38,39] However, when non-human primates were injected with AAV-PHP.B, broad CNS transduction was achieved only following intracisternal administration, not intravascular delivery.[39–41]

In the cat brain, intraparenchymal injection of AAV1 produced superior spread of transduction from the injection site compared to AAV2, and no neuronal transduction occurred with AAV5.[42] In a feline model of alpha-mannosidosis, intraparenchymal injection of AAV1-fMANB produced widespread but incomplete correction in the brain and improvement of clinical disease.[26] While promising, this strategy

Received 17 December 2021; accepted 12 July 2022;
https://doi.org/10.1016/j.omtm.2022.07.007.

[5]Present address: Center for Gene Therapy, Abigail Wexner Research Institute, Nationwide Children's Hospital, Columbus, OH 43205, USA

Correspondence: John H. Wolfe, Children's Hospital of Philadelphia, 502-G Abramson Research Center, 3615 Civic Center Boulevard, Philadelphia, PA 19104-4399, USA.
E-mail: jhwolfe@vet.upenn.edu

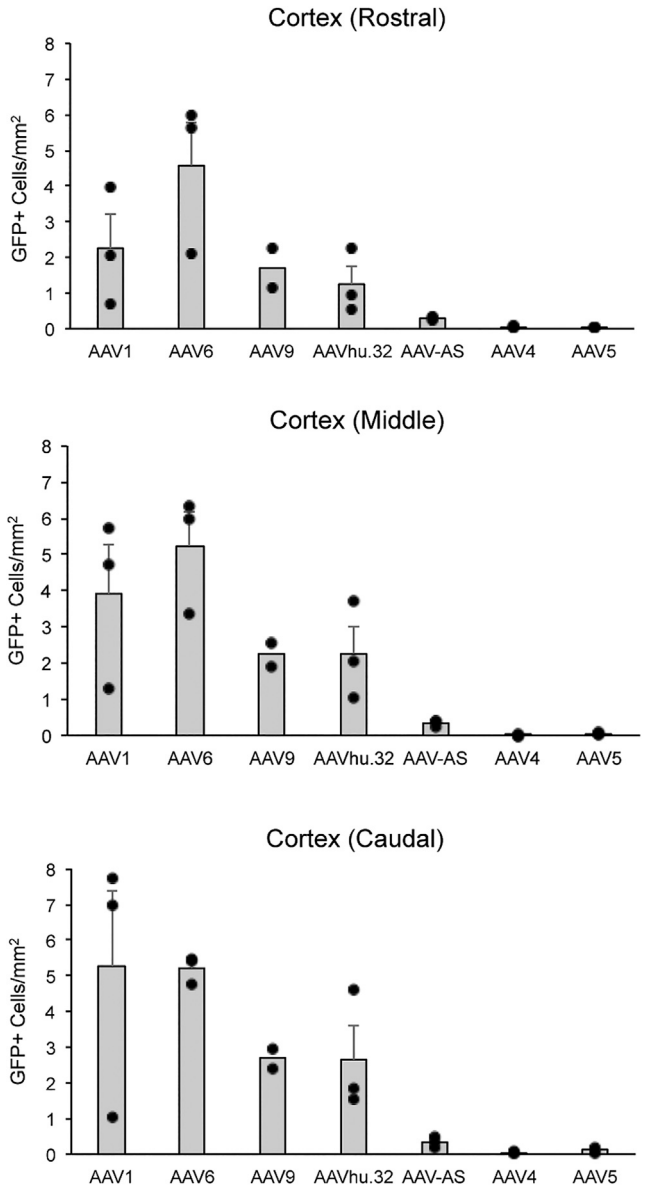

Figure 1. Comparison of GFP expression in the feline cerebral cortex following intracisternal injection of multiple AAV serotypes

Normal 4-week-old cats (n = 2 for AAV9; n = 3 for all other vectors) received *cisterna magna* injections of 1×10^{13} vg vector encoding EGFP. GFP-expressing cells were counted at multiple points along the rostral-caudal axis following DAB immunohistochemistry for EGFP at 4 weeks post-injection. Values are expressed as number of GFP-expressing cells per square millimeter. Bars represent means + SEMs.

would require injecting a large number of tracks to achieve the widespread gene transfer needed to treat a human brain.[1,26,39,43] An alternative to the intraparenchymal route is injection into the *cisterna magna* (CM), which is a simple procedure and less invasive than injecting vectors along multiple injection tracks. Delivery of AAV into the CSF results in circulation of the vector within the brain and can achieve widespread CNS transduction.[31] This route of administration circumvents the blood-brain barrier and may allow lower total doses to be used compared to intravascular delivery.

In the present study, we evaluated alternative AAV serotypes for patterns of transduction after CSF delivery. The cat was chosen for this study due to the gyrencephalic structure of the cat brain, and because it is a well-established model for neurological studies. Three of the serotypes tested are closely related to AAV1 and AAV9, which have been effective in the cat brain.[31] We also evaluated two serotypes that transduce choroid plexus epithelial (CPE) and ependymal cells in rodent models, which may allow for secretion of high levels of therapeutic protein into CSF circulation. In the cat brain, intracisternal delivery of AAV1 produced widespread transduction and clinical improvement in a feline model of alpha-mannosidosis.[31] AAV6 is closely related to AAV1 and produces a similar transduction profile, including reaching multiple layers of the cerebral cortex, the choroid plexus and ependyma, and some deeper structures of the brain. Serotypes AAVhu.32 and AAV-AS are closely related to AAV9 and produce transduction profiles similar to AAV9. Serotypes AAV4 and AAV5 primarily transduce the CPE and ependymal cells in the mouse brain, but only AAV4 was observed to do so in the cat brain. These data are useful for targeting gene transduction to specific target areas in experimental models with large brains.

RESULTS

Alternative AAV serotypes were tested with the goal of identifying those with improved transduction characteristics compared to the previously studied AAV1 and AAV9.[31] AAV6 was chosen as it is closely related to AAV1 (clade A) and is thought to be derived from a recombination between AAV1 and AAV2.[44] AAV1 produces widespread transduction of gray matter, choroid plexus, ependyma, and some transduction of glia in white matter.[31] Serotype AAVhu.32 was chosen as it belongs to the same clade as AAV9 (clade F), which produces widespread CNS transduction following CM injection but less efficiently than AAV1.[31] Both AAV9 and AAVhu.32 can mediate axonal transport of the vector genome within the brain,[20,22,45] as well as cross the blood-brain barrier after intravascular injection.[34] AAV-AS was generated by the modification of the AAV9.47 capsid and mediates widespread CNS transduction in the mouse and cat after direct injection.[46] Serotypes AAV4 and AAV5 were selected based on their ability to transduce CPE and ependymal cells in the mouse brain,[16,19,47–49] which are potential targets for expressing high levels of secreted proteins into CSF circulation.

Normal cats were injected intracisternally at 4 weeks of age, with AAV vectors containing a genome consisting of a human β-glucuronidase (hGUSB) promoter-driven enhanced GFP (EGFP).[50] The hGUSB promoter was chosen as it is a mammalian pan-cellular promoter whose small size (378 bp) allows for its use with larger transgenes and is expressed in all tissues and in multiple species. A total of 1×10^{13} vector genome copies were delivered to each animal. Cats were euthanized 4 weeks after injection and the brains were perfused with PBS, removed, paraformaldehyde fixed, frozen, and sectioned coronally. No cats showed any abnormal clinical signs during the 4-week period of the study and serum chemistry values taken pre-euthanasia were normal

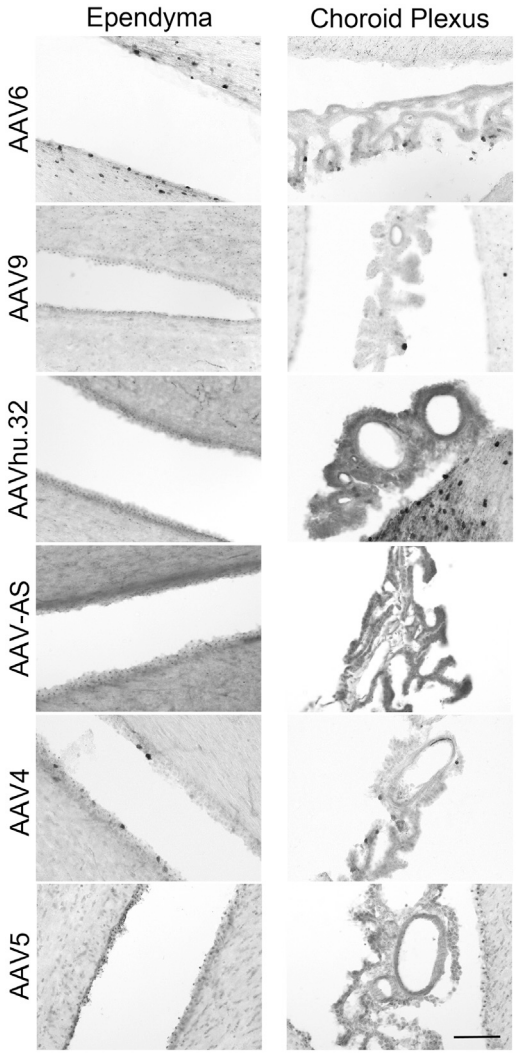

Figure 2. Multiple AAV serotypes transduce CSF-producing cells following intracisternal injection

Normal 4-week-old cats (n = 2 for AAV9; n = 3 for all other vectors) received *cisterna magna* injections of 1×10^{13} vg vector encoding EGFP. Vector transduction of choroid plexus and ependymal cells were analyzed by immunohistochemistry for EGFP at 4 weeks post-injection. Images shown are representative examples from each serotype. Scale bar, 100 μm.

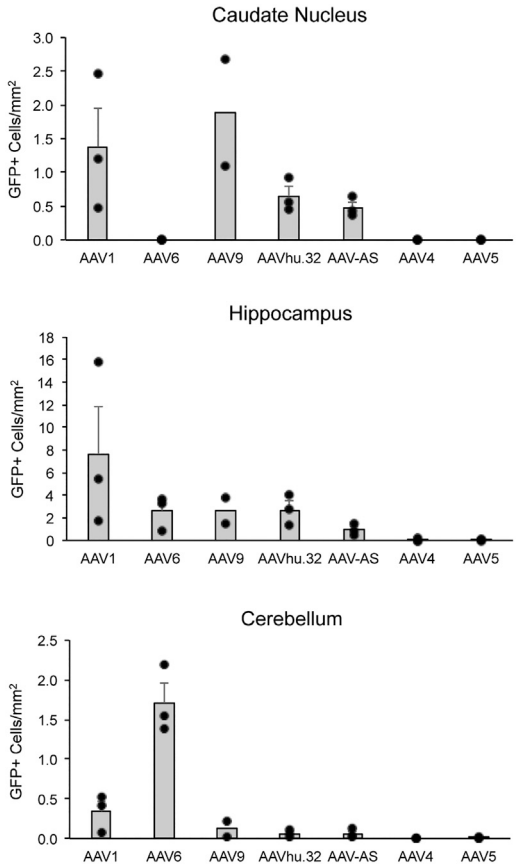

Figure 3. Transduction of other brain structures by multiple AAV serotypes following intracisternal injection

Normal 4-week-old cats (n = 2 for AAV9; n = 3 for all other vectors) received *cisterna magna* injections of 1×10^{13} vg vector encoding EGFP. GFP-expressing cells in specific structures within the brain were counted following DAB immunohistochemistry for EGFP at 4 weeks post-injection. Values are expressed as number of GFP-expressing cells per square millimeter. Bars represent means + SEMs.

(Table S1). AAV6 produced the greatest number of EGFP$^+$ cells, transducing cells not only in the gray matter but also the CPE and ependymal cells lining the ventricles. Of the other serotypes tested, AAVhu.32 and AAV-AS primarily transduced cells in the gray matter, and AAV4 primarily transduced CPE and ependymal cells.

Distribution in the cerebral cortex

Our previous study comparing transduction patterns of AAV1-EGFP and AAV9-EGFP in the cat brain demonstrated that AAV1 was superior to AAV9 with respect to number of cells transduced.[31] In the present study, AAV6-EGFP produced numerous EGFP$^+$ cells in the cerebral cortex throughout the rostral-caudal axis (Figure 1). Positive cells were observed in multiple layers of the cortex, and most of the positive cells were morphologically equivalent to pyramidal neurons. This transduction pattern was comparable to what we observed previously for AAV1.[31] AAVhu.32 and AAV-AS injections also produced EGFP$^+$ cells in the cortex, although fewer than AAV6, and did not appear to penetrate into the deeper layers of the cortex. When comparing these two serotypes to each other, hu.32 had a transduction pattern similar to what was observed for AAV9, while fewer transduced cells were observed with AS. In contrast to what was seen for the other serotypes, AAV4 and AAV5 resulted in a relative absence of EGFP$^+$ cells in the cortex. Representative DAB-stained sections can be viewed in Figure S1.

Distribution in CSF-secreting cells

In addition to broad transduction of neurons throughout the cortex, it is of interest to identify serotype(s) capable of transducing CSF-secreting

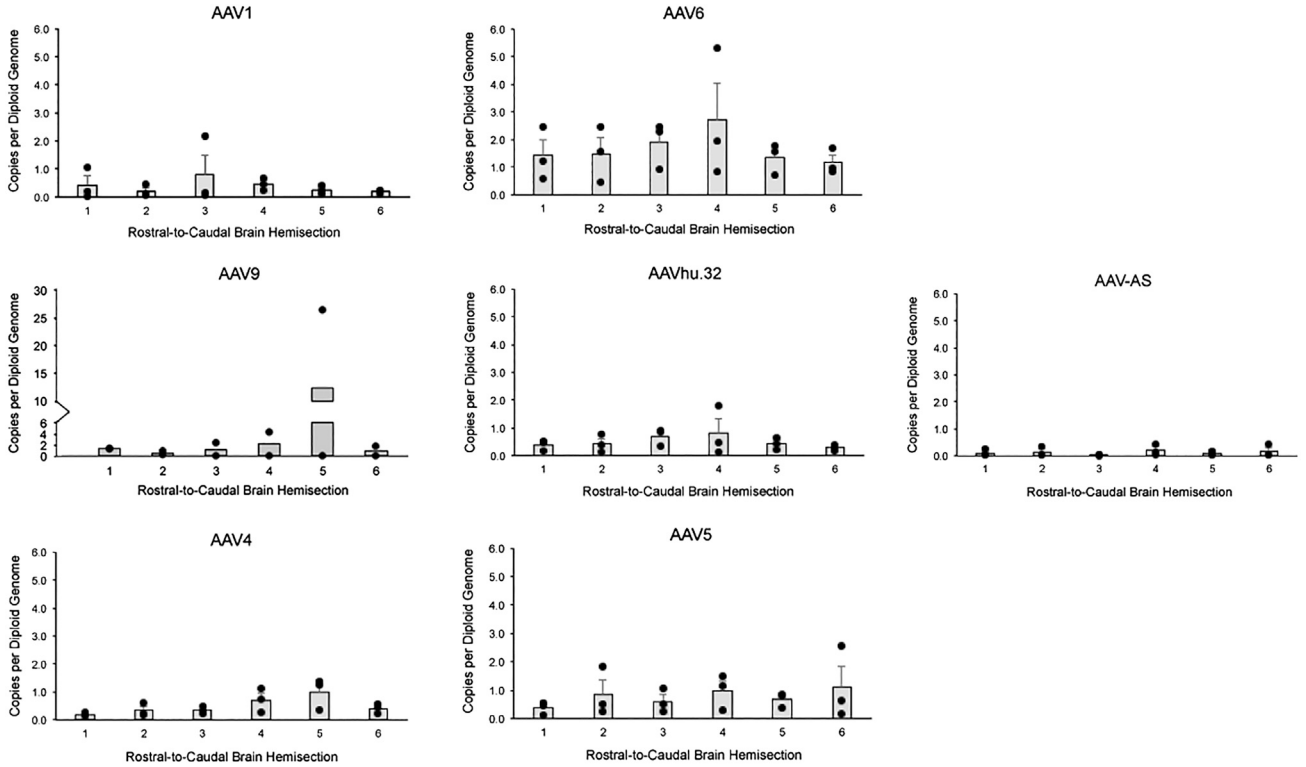

Figure 4. Quantification of vector genome copies following intracisternal injection of multiple AAV serotypes

qPCR was performed to assess distribution of vector genome copies in the brain. Tissues samples were taken from multiple sites along the rostral-to-caudal axis. Values are expressed as vector genome copies per diploid cell genome (n = 2 for AAV9; n = 3 for all other vectors). Bars represent means + SEMs.

ependymal and CPE cells. The expression of transgenes in these structures may allow for continuous secretion of vector-encoded proteins into the CSF, potentially allowing for greater dispersal throughout the brain. AAV1 can transduce CPE and ependymal cells in mice and cats.[18,31] The closely related AAV6 produced similar results, with EGFP$^+$ cells being identified in the choroid plexus and in cells lining the ventricles of AAV6-injected brains (Figure 2). No EGFP$^+$ CPE or ependymal cells were detected for AAVhu.32 or AAV-AS (Figure 2); however, a few EGFP$^+$ cells were identified in the choroid plexus of AAV9-injected animals (Figure 2). Transduced EGFP$^+$ CPE and ependymal cells were observed with AAV4 but not AAV5 (Figure 2). This is consistent with what other groups have reported in the mouse for AAV4 but in contrast with reports for AAV5.[16,19,47,49]

Distribution in sub-cortical structures

Transduction of other major brain structures may be important clinically for treating lysosomal storage diseases because the pathology is found throughout the brain. AAV1 transduces the hippocampus and caudate nucleus in the cat brain.[31] In the AAV6-injected animals, transduction was observed predominantly in cells with the morphology of granule cells in the hippocampus and Purkinje cells in the cerebellum (Figure 3). Positive cells were mostly absent from the caudate nucleus, in contrast to AAV1. With either AAVhu.32 or AAV-AS, EGFP$^+$ cells were identified in the hippocampus and cerebellum, and transduced cells morphologically consistent with medium spiny neurons were found in the caudate nucleus. Similar to the cortex, a greater number of EGFP$^+$ cells were observed in the hu.32 group than in the AS group. The transduction pattern for hu.32 was similar to what was observed for AAV9. Few, if any, transduced cells were found in any of the regions examined for AAV4 or AAV5. Representative DAB-stained sections are shown in Figure S2.

To support the immunohistology data, we determined the number of vector genomes present in multiple sections along the rostral-caudal axis. Six hemi-sections along the rostral-caudal axis were analyzed (Figure 4). Overall, greater copy numbers were observed in AAV6-injected sections. Surprisingly, vector genome copies measured for the AAV4- and AAV5-injected sections were comparable to those from the AAVhu.32-injected sections, despite producing far fewer EGFP$^+$ cells in our immunohistochemical studies.

Spinal cord

Many neurological diseases also affect the spinal cord; therefore, transduction of both parts of the CNS would be beneficial for any potential therapy. Delivery of vector into the CSF via intracisternal injection should allow for the transduction of both brain and spinal cord, which was demonstrated previously for AAV1 and AAV9 in multiple species.[25,31,51–53] The transduction characteristics of our panel of

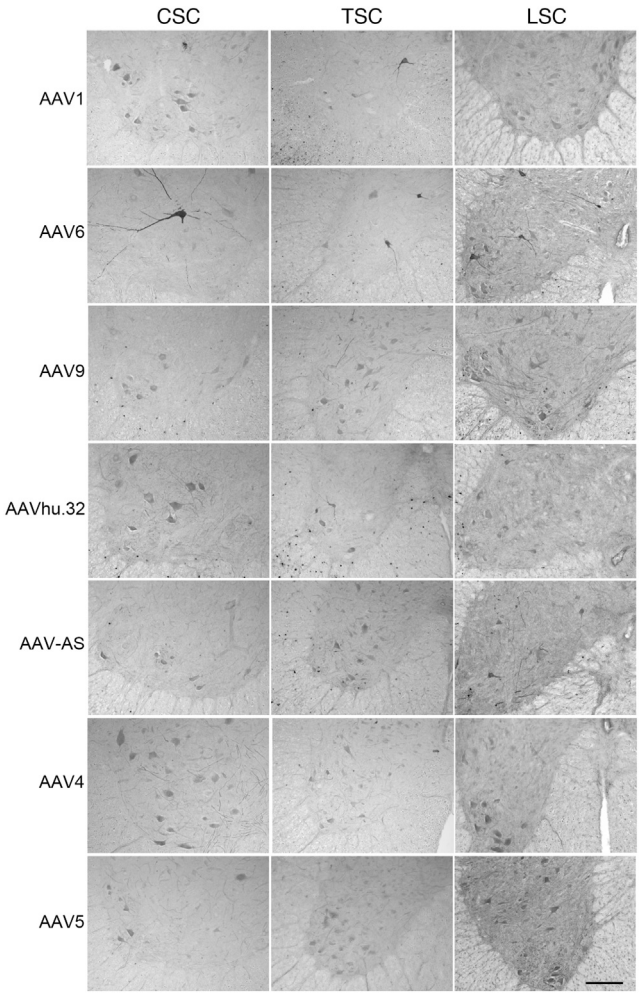

Figure 5. Transduction of motor neurons of the anterior horn of the spinal cord following intracisternal delivery of different AAV serotypes

Normal 4-week-old cats (n = 1 for AAV1 and AAV9; n = 3 for all other vectors) received *cisterna magna* injections of 1×10^{13} vg vector encoding EGFP. Vector transduction of cervical (CSC), thoracic (TSC), and lumbar (LSC) spinal cord sections were analyzed by immunohistochemistry for EGFP at 4 weeks post-injection. Images shown are representative examples from each serotype. Scale bar, 200 μm.

AAV serotypes in the spinal cord was determined using immunohistochemical staining on sections from the cervical, thoracic, and lumbar regions. All five serotypes transduced motor neurons in the gray matter of the ventral horn (Figure 5). qPCR analysis of cervical, thoracic, and lumbar sections showed the overall greatest number of vector genome copies in sections from animals injected with AAVhu.32, with elevated vector genome copies in the lumbar sections for AAV4 and AAV6 (Figure S3).

Biodistribution of AAV serotypes outside the CNS

As CSF circulates through the brain and spinal cord, it is eventually reabsorbed into the bloodstream, allowing waste to be removed from the brain.[54,55] Therefore, it is likely that any vector not taken up by cells in the CNS circulates throughout the body, allowing for the transduction of distal organs. In the case of neurometabolic diseases, such as lysosomal storage diseases, the genetic defect is present in all cells. Although the organs and severity of pathology vary among the different types of LSDs, any correction that occurs outside the CNS would be beneficial clinically.

Some transduction of non-CNS organs was observed for all serotypes tested. AAV6 transduced cells in the liver and spleen (Figure 6), whereas $EGFP^+$ cells were detected in the liver, kidney, and spleen of animals injected with AAVhu.32 (Figure 6). While CNS transduction by AAV-AS largely followed the same pattern as hu.32, $EGFP^+$ cells were detected only in the liver in AAV-AS-injected animals, and to a lesser extent than hu.32 (Figure 6). Minimal transduction of organs outside the CNS was observed for AAV4 (Figure 6) or AAV5 (Figure 6), primarily in the spleen and lung. No transduction of heart or muscle was observed for any serotype (data not shown). Consistent with the immunohistochemical findings, the measurement of genome copies in the different tissues showed the highest amount of vector genome in the livers of animals injected with either AAVhu.32 or AAV-AS (Figure 7). Vector genome copies were detected in the heart and muscle of some animals, despite the immunohistochemistry of these organs appearing negative.

Summary of findings

Of the new serotypes tested, AAV6 produced the greatest number of $EGFP^+$cells, transducing cells in the gray matter as well as in the CPE and ependymal cells lining the ventricles. The potential advantage of targeting these cells is that they secrete large amounts of protein in generating the CSF.[49] The distribution of cells transduced with AAV6 was similar to that seen with the closely related AAV1 serotype.[31] The serotypes closely related to AAV9, AAVhu.32 and AAV-AS, primarily transduced cells in the gray matter by CM delivery. AAV9 and AAVhu.32 can also mediate transduction of the brain by crossing the blood-brain barrier.[1,34,37] However, AAVhu.32 to date is the only vector shown to completely correct the brain in a large animal model of a human disease.[38] AAV4 primarily transduced CPE and ependymal cells.

DISCUSSION

Intracisternal vector administration has several benefits: It is less invasive than multiple injection tracks throughout the brain; it is more specific to the CNS than intravascular delivery; and it circumvents the blood-brain barrier. Knowledge of transduction characteristics is critical for targeting specific structures of the whole brain, and while much is known about the transduction characteristics of many serotypes in the rodent brain, more data are needed for the transduction characteristics of various serotypes in the large animal brain. While our laboratory previously identified that AAV1 can produce widespread transduction in the cat brain leading to clinical improvement in an alpha-mannosidosis cat model,[31] the goal of the present study was to identify additional AAV serotype(s) that could provide more widespread transduction of neural cells in multiple structures of a large animal brain.

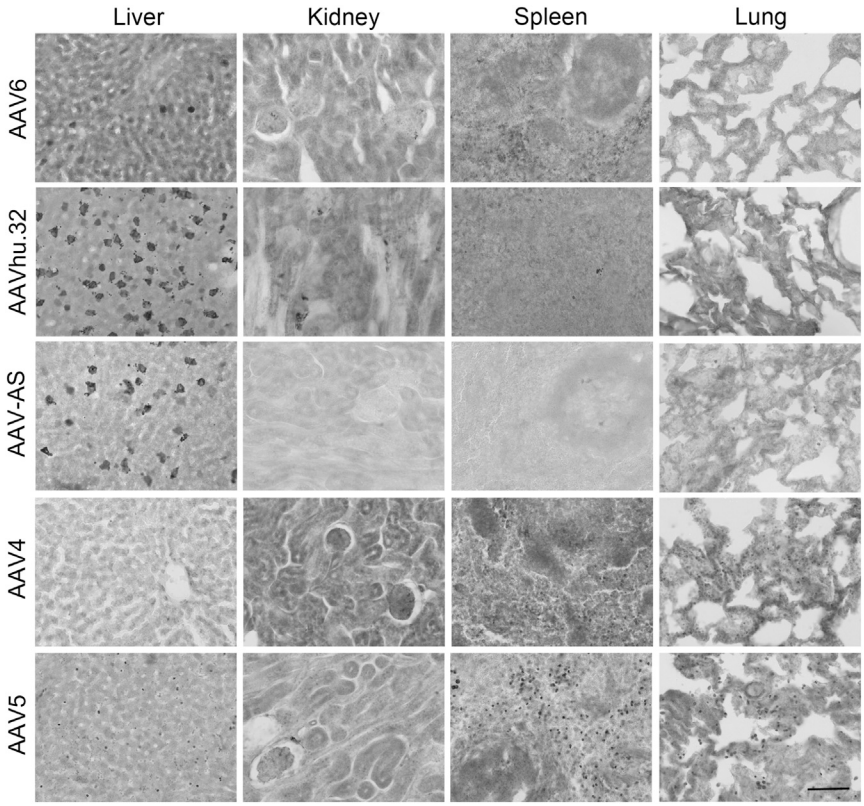

Figure 6. Differential transduction of peripheral organs by multiple AAV serotypes following intracisternal injection

Normal 4-week-old cats (n = 3 per vector) received *cisterna magna* injections of 1×10^{13} vg vector encoding EGFP. Vector transduction of multiple peripheral organs was analyzed by immunohistochemistry for EGFP at 4 weeks post-injection. Images shown are representative examples from each serotype. Scale bar, 100 μm.

We observed significant differences in the transduction profiles between the serotypes tested, with closely related serotypes having similar profiles. Of the serotypes tested, AAV6 transduced the greatest number of cortical neurons in multiple layers of the cortex, the choroid plexus, and ependymal cells lining the ventricles. This transduction pattern was similar to that previously observed for AAV1,[31] a serotype belonging to the same clade as AAV6. Minimal transduction of the liver and spleen was also observed. AAVhu.32 transduced cortical neurons and multiple deeper brain structures but lacked transduction of CSF-producing cells. This transduction profile is similar to that observed previously in AAV9-injected cats.[31] The overall similarity between AAVhu.32 and AAV9 transduction profiles is also similar to the patterns in mice.[22] AAVhu.32 also produced transduction of multiple peripheral organs. AAV-AS had a transduction profile similar to that of hu.32, however fewer $EGFP^+$ cells were observed in all of the tissues examined. The distribution of GFP-expressing cells in different hemisections along the rostral-to-caudal axis for the serotypes tested can be found in Figure S4. Table S2 contains the relative EGFP expression for all of the serotypes tested in the cortex and a selection of other brain structures.

The injection of AAV4 and AAV5 into the CSF was directed at transducing CPE and ventricular lining cells based on previous studies in mice.[42–45] Although low in density, the AAV4-injected cats had $EGFP^+$cells in the choroid plexus, ependyma, and spinal cord. While this was consistent with studies in mice,[16,47,49] AAV4 failed to transduce the ependyma in the canine brain.[56]

The lack of transduction by AAV5 in the cat is consistent with previous findings after direct intraparenchymal injection in the cat.[42] However, this is not a general finding in large animal models since AAV5-GFP transduces glia in non-human primates following intraparenchymal injection.[57,58] Although it is not clear why AAV5 transduces the cat brain so poorly as compared to other species, sequence differences in the feline platelet-derived growth factor receptor α (PDGFRα) and AAVR receptors, which are implicated in AAV5 transduction,[59–62] may explain this anomaly. The feline sequences for these receptors differ from other large animal species in the extracellular immunoglobulin (Ig)-like domains of PDGFRα (Figure S5), although it is not known whether these sites are required for AAV5 transduction. There are also sequence differences in the feline AAVR PKD1 domain (Figure S5), which is required for AAV5 transduction.[61,62] These proteins are probably functional since there is no evidence to indicate that they are defective in normal cats. The qPCR experiments detected vector genomes in the AAV5 group at a level comparable to several of the other serotypes tested. It is possible that the assay is detecting fragments of the vector genome, rather than the full genome sequence or extracellular vector.

We did not observe any sign of cytotoxic response in any of the brain sections analyzed in this study, although the present study was done at a relatively moderate titer. Some recent studies have found increased risks of cytotoxic responses to non-self-proteins such as GFP, however these occurred at very high vector titers.[63–66] This may be less of a problem in a therapeutic setting, depending on the nature of the therapeutic protein. In most of the LSDs, the extracellular therapeutic protein that is secreted from a transduced cell is taken up by neighboring cells (cross-correction) to restore catabolism. This results in a greater number of cells being functionally corrected than are transduced. Therefore, delivery efficiency does not need to be high to produce a beneficial effect.

Intracisternal injection of the AAV serotypes used in this study produced distinct transduction patterns in the cat brain, with similarities

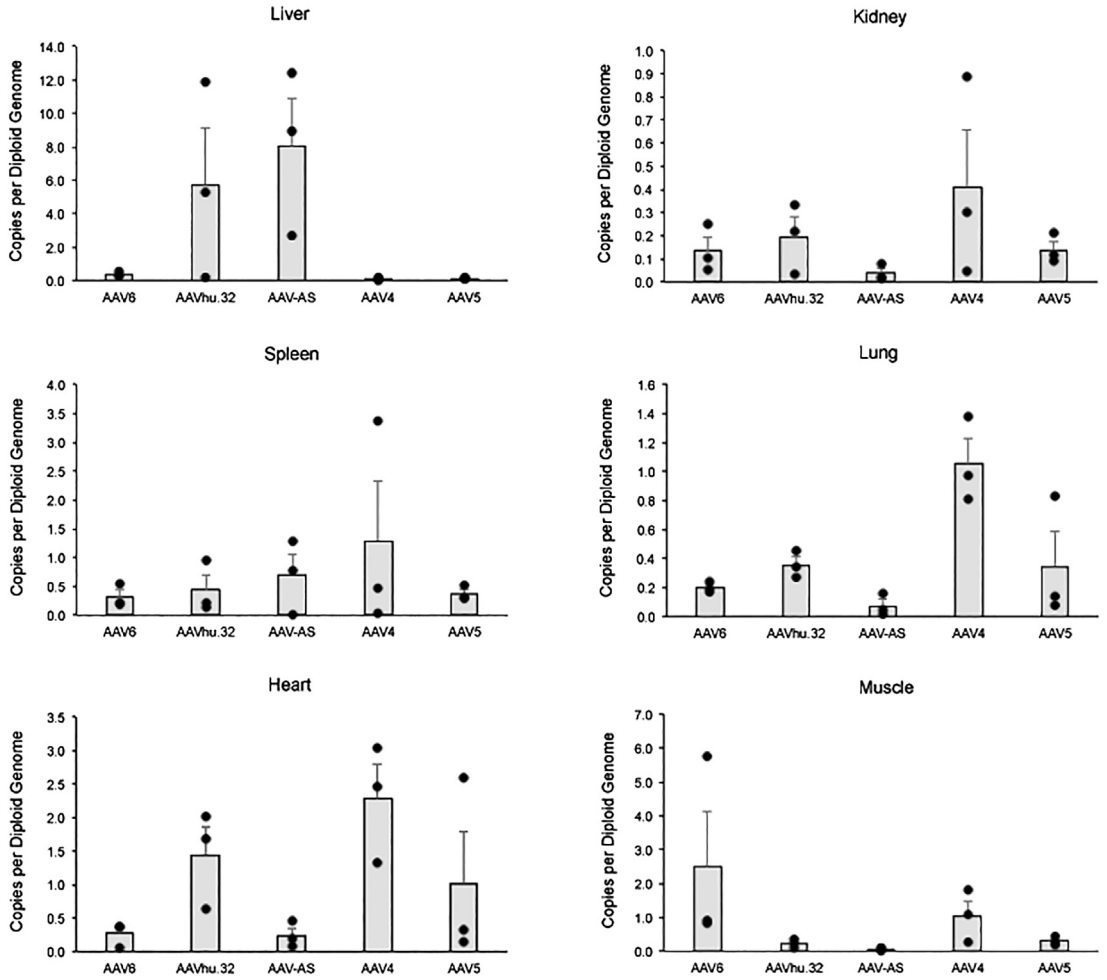

Figure 7. Quantification of vector genome copies in select peripheral organs following intracisternal injection of multiple AAV serotypes

qPCR was performed to assess distribution of vector genome copies in peripheral organs. Values are expressed as vector genome copies per diploid cell genome. n = 3 per vector. Bars represent means + SEMs.

between serotypes within the same clade. Serotypes AAV6 (this study) and AAV1[36] are the most capable of widespread transduction of the cortex by CSF delivery, which may be critical for treating neurocognitive deficiencies.

MATERIALS AND METHODS

Plasmid and AAV production

The EGFP gene was cloned into the AAV packaging plasmid pZac2.1, provided by the Vector Core of the University of Pennsylvania. The vector genome contained AAV2 terminal repeats, a human GUSB promoter, simian virus 40 splice donor/acceptor signal, and bovine growth hormone polyadenylation signal. AAV4 and AAV-AS capsid plasmids were provided by J. Chiorini and M. Sena-Esteves, respectively. Recombinant AAV vectors of all of the serotypes were packaged as a single-stranded AAV (ssAAV) genome by the University of Pennsylvania Vector Core following triple (AAV1, AAV5, AAV6, AAV9, AAVhu.32) or quadruple (AAV-AS, AAV4) transfection of HEK293 cells by AAV cis-plasmid, AAV trans-plasmid containing AAV rep and cap genes, and adenovirus helper plasmid. Vectors were purified using iodixanol gradient ultracentrifugation, and the titers were determined by real-time PCR.[67] All of the vectors were prepared and titered using the same methods. Titers were adjusted to 1×10^{13} vg/mL before use.

Animals and vector injections

All of the animal care and procedures were in accordance with the Institutional Animal Care and Use Committee at the University of Pennsylvania. Normal cats (4 weeks old) produced in the breeding colony of the University of Pennsylvania veterinary school were used for experiments. Cats were anesthetized with intravenous propofol (up to 6 mg/kg). A catheter was placed in the cephalic vein, and enough propofol was given to allow intubation. Animals were positioned in right-side lateral recumbency and were anesthetized during the procedure. Using sterile techniques, approximately

0.5 mL CSF was collected using a 22-G spinal needle from the cerebellomedullary cistern. After collecting the CSF, 1×10^{13} genome copies of vector in 1.0 mL total volume were injected over the course of 1 min, with a dwell time of approximately 5 s. Heart and respiratory rates were monitored until fully recovered. All of the animals were injected at the same age, by the same staff, and using the same procedure.

Tissue collection

Four weeks post-injection, cats were euthanized by using an overdose of intravenous barbiturates. After sacrifice, cats were transcardially perfused with 700 mL of 0.9% cold saline and tissues were drop fixed in 4% paraformaldehyde for 48 h. For cryosectioning, brains were cryoprotected in 30% sucrose, embedded in optimum cutting temperature solution (Sakura, Torrance, CA, USA), and then cryosectioned at 20–40 μm thickness using a cryostat (Leica Microsystems, Wetzlar, Germany) for subsequent immunohistochemical staining or guide DNA (gDNA) isolation. For serum collection, the whole blood was incubated for 30 min at room temperature followed by centrifugation at 1,000 × *g* for 15 min. The supernatant was then aspirated and stored at −80°C. All of the sera were tested by the University of Pennsylvania Clinical Pathology Laboratory.

Immunohistochemistry

GFP^+ cells were labeled using DAB immunohistochemistry. Frozen sections were permeabilized and immunoblocked for 30 min in 4% goat serum in PBS-T (PBS containing 0.3% Triton X-100). The sections were then incubated overnight at 4°C with the rabbit anti-GFP (1:1,000, A11122, Thermo Fisher, Austin, TX, USA). After three washes in PBS-T, sections were incubated with a biotinylated goat anti-rabbit secondary antibody (1:250, Vector Laboratories, Burlingame, CA, USA) for 45 min followed by PBS-T washes. The antibody binding was visualized using VECTASTAIN Elite ABC reagent (Vector Laboratories) and 3,3′-diaminobenzidine substrate kit for peroxidase (Vector Laboratories). Sections were then dehydrated and mounted in DPX mounting medium (Sigma, St. Louis, MO, USA) with glass coverslips. Images were visualized using a Leica AF6000 LX microscope (Leica, Heerbrugg, Switzerland) and acquired using a DFC 425 digital camera (Leica, Heerbrugg, Switzerland).

GFP-expressing cells were quantified in DAB-stained cat brain hemisections. Images were converted to grayscale, and an identical threshold was applied. The number of cells in the sections over the set threshold was counted by particle analysis, and the area of brain sections or specific brain regions were measured using ImageJ software (NIH, Bethesda, MD, USA).

Quantification of vector genomes

Viral genome copies present in tissues were determined using quantitative real-time PCR. Genomic DNA was extracted from two to three 40-μm sections of each transverse brain block and vector genome copies were quantified. For peripheral organs, approximately 10 mg of tissue was used to extract genomic DNA. Copies of EGFP vector genome were quantified using PowerUp SYBR Green Master Mix (Thermo Fisher). Triplicate samples derived from each DNA pool were used for quantification. The primer sequences were as follows: forward: 5′-CTGGACGGCGACGTAAAC-3′, reverse: 5′-GAACTTC AGGGTCAGCTTGC-3′.

DATA AVAILABILITY

All data and supporting materials are available within the article and supplemental information. Raw data can be provided by the corresponding author on reasonable request.

SUPPLEMENTAL INFORMATION

Supplemental information can be found online at https://doi.org/10.1016/j.omtm.2022.07.007.

ACKNOWLEDGMENTS

We thank M. Parente, A. Polesky, and C. Cross for expert technical assistance. This work was supported by NIH grants R01-NS110349, P40-OD010939, and U01-HD079066.

AUTHOR CONTRIBUTIONS

J.E.H., S.G.K., and J.H.W. designed the experiments; C.M.M., J.H.B., and P.A.O. performed injections and provided medical management; J.E.H. performed immunohistochemistry and PCR experiments; J.E.H. and J.H.W. analyzed the data and wrote the manuscript.

DECLARATION OF INTERESTS

The authors declare no competing interests.

REFERENCES

1. Simonato, M., Bennett, J., Boulis, N.M., Castro, M.G., Fink, D.J., Goins, W.F., Gray, S.J., Lowenstein, P.R., Vandenberghe, L.H., Wilson, T.J., et al. (2013). Progress in gene therapy for neurological disorders. Nat. Rev. Neurol. *9*, 277–291.

2. Kakkis, E., McEntee, M., Vogler, C., Le, S., Levy, B., Belichenko, P., Mobley, W., Dickson, P., Hanson, S., and Passage, M. (2004). Intrathecal enzyme replacement therapy reduces lysosomal storage in the brain and meninges of the canine model of MPS I. Mol. Genet. Metab. *83*, 163–174.

3. Hemsley, K.M., King, B., and Hopwood, J.J. (2007). Injection of recombinant human sulfamidase into the CSF via the cerebellomedullary cistern in MPS IIIA mice. Mol. Genet. Metab. *90*, 313–328.

4. Lee, W.C., Tsoi, Y.K., Troendle, F.J., DeLucia, M.W., Ahmed, Z., Dicky, C.A., Dickson, D.W., and Eckman, C.B. (2007). Single-dose intracerebroventricular administration of galactocerebrosidase improves survival in a mouse model of globoid cell leukodystrophy. Faseb. J. *21*, 2520–2527.

5. Chang, M., Cooper, J.D., Sleat, D.E., Cheng, S.H., Dodge, J.C., Passini, M.A., Lobel, P., and Davidson, B.L. (2008). Intraventricular enzyme replacement improves disease phenotypes in a mouse model of late infantile neuronal ceroid lipofuscinosis. Mol. Ther. *16*, 649–656.

6. Dodge, J.C., Clarke, J., Treleaven, C.M., Taksir, T.V., Griffiths, D.A., Yang, W., Fidler, J.A., Passini, M.A., Karey, K.P., Schuchman, E.H., et al. (2009). Intracerebroventricular infusion of acid sphingomyelinase corrects CNS manifestations in a mouse model of Niemann-Pick A disease. Exp. Neurol. *215*, 349–357.

7. Auclair, D., Finnie, J., White, J., Nielsen, T., Fuller, M., Kakkis, E., Cheng, A., O'Neill, C.A., and Hopwood, J.J. (2010). Repeated intrathecal injections of recombinant human 4-sulphatase remove dural storage in mature mucopolysaccharidosis VI cats primed with a short-course tolerisation regimen. Mol. Genet. Metab. *99*, 132–141.

8. Dierenfeld, A.D., McEntee, M.F., Vogler, C.A., Vite, C.H., Chen, A.H., Passage, M., Le, S., Shah, S., Jens, J.K., Snella, E.M., et al. (2010). Replacing the enzyme

α-L-iduronidase at birth ameliorates symptoms in the brain and periphery of dogs with mucopolysaccharidosis type I. Sci. Transl. Med. *2*, 60ra89.

9. Crawley, A.C., Marshall, N., Beard, H., Hassiotis, S., Walsh, V., King, B., Hucker, N., Fuller, M., Jolly, R.D., Hopwood, J.J., and Hemsley, K.M. (2011). Enzyme replacement reduces neuropathology in MPS IIIA dogs. Neurobiol. Dis. *43*, 422–434.

10. Vera, M., Le, S., Kan, S.-H., Garban, H., Naylor, D., Mlikotic, A., Kaitila, I., Harmatz, P., Chen, A., and Dickson, P. (2013). Immune response to intrathecal enzyme replacement therapy in mucopolysaccharidosis I patients. Pediatr. Res. *74*, 712–720.

11. Lu, J.-Y., Nelvagal, H.R., Wang, L., Birnbaum, S.G., Cooper, J.D., and Hofmann, S.L. (2015). Intrathecal enzyme replacement therapy improves motor function and survival in a preclinical mouse model of infantile neuronal ceroid lipofuscinosis. Mol. Genet. Metab. *116*, 98–105.

12. Wiseman, J.A., Meng, Y., Nemtsova, Y., Matteson, P.G., Millonig, J.H., Moore, D.F., Sleat, D.E., and Lobel, P. (2017). Chronic enzyme replacement to the brain of a late infantile neuronal ceroid lipofuscinosis mouse has differential effects on phenotypes of disease. Mol. Ther. Methods Clin. Dev. *4*, 204–212.

13. Sohn, Y.B., Ko, A.-R., Seong, M.-R., Lee, S., Kim, M.R., Cho, S.Y., Kim, J.-S., Sakaguchi, M., Nakazawa, T., Kosuga, M., et al. (2018). The efficacy of intracerebroventricular idursulfase-beta enzyme replacement therapy in mucopolysaccharidosis II murine model: heparan sulfate in cerebrospinal fluid as a clinical biomarker of neuropathology. J. Inherit. Metab. Dis. *41*, 1235–1246.

14. Eisengart, J.B., Pierpont, E.I., Kaizer, A.M., Rudser, K.D., King, K.E., Pasquali, M., Polgreen, L.E., Dickson, P.I., Le, S.Q., Miller, W.P., et al. (2019). Intrathecal enzyme replacement for Hurler syndrome: biomarker association with neurocognitive outcomes. Genet. Med. *21*, 2552–2560.

15. Skorupa, A.F., Fisher, K.J., Wilson, J.M., Parente, M.K., and Wolfe, J.H. (1999). Sustained production of beta-glucuronidase from localized sites after AAV vector gene transfer results in widespread distribution of enzyme and reversal of lysosomal storage lesions in a large volume of brain in mucopolysaccharidosis VII mice. Exp. Neurol. *160*, 17–27.

16. Davidson, B.L., Stein, C.S., Heth, J.A., Martins, I., Kotin, R.M., Derksen, T.A., Zabner, J., Ghodsi, A., and Chiorini, J.A. (2000). Recombinant adeno-associated virus type 2, 4, and 5 vectors: transduction of variant cell types and regions in the mammalian central nervous system. Proc. Natl. Acad. Sci. USA *97*, 3428–3432.

17. Heuer, G.G., Passini, M.A., Jiang, K., Parente, M.K., Lee, V.M.-Y., Trojanowski, J.Q., and Wolfe, J.H. (2002). Selective neurodegeneration in murine mucopolysaccharidosis VII is progressive and reversible. Ann. Neurol. *52*, 762–770.

18. Passini, M.A., Watson, D.J., Vite, C.H., Landsburg, D.J., Feigenbaum, A.L., and Wolfe, J.H. (2003). Intraventricular brain injection of adeno-associated virus type 1 (AAV1) in neonatal mice results in complementary patterns of neuronal transduction to AAV2 and total long-term correction of storage lesions in the brains of β-glucuronidase-deficient mice. J. Virol. *77*, 7034–7040.

19. Liu, G., Martins, I., Wemmie, J.A., Chiorini, J.A., and Davidson, B.L. (2005). Functional correction of CNS phenotypes in a lysosomal storage disease model using adeno-associated virus type 4 vectors. J. Neurosci. *25*, 9321–9327.

20. Cearley, C.N., and Wolfe, J.H. (2006). Transduction characteristics of adeno-associated virus vectors expressing cap serotypes 7, 8, 9, and Rh10 in the mouse brain. Mol. Ther. *13*, 528–537.

21. Taymans, J.-M., Vandenberghe, L.H., Haute, C.V.D., Thiry, I., Deroose, C.M., Mortelmans, L., Wilson, J.M., Debyser, Z., and Baekelandt, V. (2007). Comparative analysis of adeno-associated viral vector serotypes 1, 2, 5, 7, and 8 in mouse brain. Hum. Gene Ther. *18*, 195–206.

22. Cearley, C.N., Vandenberghe, L.H., Parente, M.K., Carnish, E.R., Wilson, J.M., and Wolfe, J.H. (2008). Expanded repertoire of AAV vector serotypes mediate unique patterns of transduction in mouse brain. Mol. Ther. *16*, 1710–1718.

23. Zincarelli, C., Soltys, S., Rengo, G., and Rabinowitz, J.E. (2008). Analysis of AAV serotypes 1-9 mediated gene expression and tropism in mice after systemic injection. Mol. Ther. *16*, 1073–1080.

24. Aschauer, D.F., Kreuz, S., and Rumpel, S. (2013). Analysis of transduction efficiency, tropism and axonal transport of AAV serotypes 1, 2, 5, 6, 8 and 9 in the mouse brain. PLoS One *8*, e76310.

25. Bailey, R.M., Rozenberg, A., and Gray, S.J. (2020). Comparison of high-dose intracisterna magna and lumbar puncture intrathecal delivery of AAV9 in mice to treat neuropathies. Brain Res. *1739*, 146832.

26. Vite, C.H., McGowan, J.C., Niogi, S.N., Passini, M.A., Drobatz, K.J., Haskins, M.E., and Wolfe, J.H. (2005). Effective gene therapy for an inherited CNS disease in a large animal model. Ann. Neurol. *57*, 355–364.

27. Ellinwood, N.M., Ausseil, J., Desmaris, N., Bigou, S., Liu, S., Jens, J.K., Snella, E.M., Mohammed, E.E.A., Thomson, C.B., Raoul, S., et al. (2011). Safe, efficient, and reproducible gene therapy of the brain in the dog models of sanfilippo and Hurler syndromes. Mol. Ther. *19*, 251–259.

28. Bradbury, A.M., Cochran, J.N., McCurdy, V.J., Johnson, A.K., Brunson, B.L., Gray-Edwards, H., Leroy, S.G., Hwang, M., Randle, A.N., Jackson, L.S., et al. (2013). Therapeutic response in feline sandhoff disease despite immunity to intracranial gene therapy. Mol. Ther. *21*, 1306–1315.

29. Hinderer, C., Bell, P., Gurda, B.L., Wang, Q., Louboutin, J.-P., Zhu, Y., Bagel, J., O'Donnell, P., Sikora, T., Ruane, T., et al. (2014). Intrathecal gene therapy corrects CNS pathology in a feline model of mucopolysaccharidosis I. Mol. Ther. *22*, 2018–2027.

30. Rockwell, H.E., McCurdy, V.J., Eaton, S.C., Wilson, D.U., Johnson, A.K., Randle, A.N., Bradbury, A.M., Gray-Edwards, H.L., Baker, H.J., Hudson, J.A., et al. (2015). AAV-mediated gene delivery in a feline model of sandhoff disease corrects lysosomal storage in the central nervous system. ASN Neuro. *7*. 1759091415569908. https://doi.org/10.1177/1759091415569908.

31. Yoon, S.Y., Bagel, J.H., O'Donnell, P.A., Vite, C.H., and Wolfe, J.H. (2016). Clinical improvement of alpha-mannosidosis cat following a single cisterna magna infusion of AAV1. Mol. Ther. *24*, 26–33.

32. Gurda, B.L., De Guilhem De Lataillade, A., Bell, P., Zhu, Y., Yu, H., Wang, P., Bagel, J., Vite, C.H., Sikora, T., Hinderer, C., et al. (2016). Evaluation of AAV-mediated gene therapy for central nervous system disease in canine mucopolysaccharidosis VII. Mol. Ther. *24*, 206–216.

33. Katz, M.L., Johnson, G.C., Leach, S.B., Williamson, B.G., Coates, J.R., Whiting, R.E.H., Vansteenkiste, D.P., and Whitney, M.S. (2017). Extraneuronal pathology in a canine model of CLN2 neuronal ceroid lipofuscinosis after intracerebroventricular gene therapy that delays neurological disease progression. Gene Ther. *24*, 215–223.

34. Yoon, S.Y., Hunter, J.E., Chawla, S., Clarke, D.L., Molony, C., O'Donnell, P.A., Bagel, J.H., Kumar, M., Poptani, H., Vite, C.H., and Wolfe, J.H. (2020). Global central nervous system correction in a large brain model of human alpha-mannosidosis by intravascular gene therapy. Brain *143*, 2058–2072.

35. Bradbury, A.M., Bagel, J.H., Nguyen, D., Lykken, E.A., Pesayco Salvador, J., Jiang, X., Swain, G.P., Assenmacher, C.A., Hendricks, I.J., Miyadera, K., et al. (2020). Krabbe disease successfully treated via monotherapy of intrathecal gene therapy. J. Clin. Invest. *130*, 4906–4920.

36. McCurdy, V.J., Johnson, A.K., Gray-Edwards, H.L., Randle, A.N., Bradbury, A.M., Morrison, N.E., Hwang, M., Baker, H.J., Cox, N.R., Sena-Esteves, M., and Martin, D.R. (2021). Therapeutic benefit after intracranial gene therapy delivered during the symptomatic stage in a feline model of Sandhoff disease. Gene Ther. *28*, 142–154.

37. Rahim, A.A., and Gissen, P. (2020). Gene therapy for global brain diseases: one small step for mice, one giant leap for humans. Brain *143*, 1964–1966.

38. Deverman, B.E., Pravdo, P.L., Simpson, B.P., Kumar, S.R., Chan, K.Y., Banerjee, A., Wu, W.L., Yang, B., Huber, N., Pasca, S.P., and Gradinaru, V. (2016). Cre-dependent selection yields AAV variants for widespread gene transfer to the adult brain. Nat. Biotechnol. *34*, 204–209.

39. Liguore, W.A., Domire, J.S., Button, D., Wang, Y., Dufour, B.D., Srinivasan, S., and McBride, J.L. (2019). AAV-PHP.B administration results in a differential pattern of CNS biodistribution in non-human primates compared with mice. Mol. Ther. *27*, 2018–2037. https://doi.org/10.1016/j.ymthe.2019.07.017.

40. Hordeaux, J., Wang, Q., Katz, N., Buza, E.L., Bell, P., and Wilson, J.M. (2018). The neurotropic properties of AAV-PHP.B are limited to C57BL/6J mice. Mol. Ther. *26*, 664–668.

41. Matsuzaki, Y., Konno, A., Mochizuki, R., Shinohara, Y., Nitta, K., Okada, Y., and Hirai, H. (2018). Intravenous administration of the adeno-associated virus-PHP.B capsid fails to upregulate transduction efficiency in the marmoset brain. Neurosci. Lett. *665*, 182–188.

42. Vite, C.H., Passini, M.A., Haskins, M.E., and Wolfe, J.H. (2003). Adeno-associated virus vector-mediated transduction in the cat brain. Gene Ther. *10*, 1874–1881.

43. Sondhi, D., Johnson, L., Purpura, K., Monette, S., Souweidane, M.M., Kaplitt, M.G., Kosofsky, B., Yohay, K., Ballon, D., Dyke, J., et al. (2012). Long-Term expression and safety of administration of AAVrh.10hCLN2 to the brain of rats and nonhuman primates for the treatment of late infantile neuronal ceroid lipofuscinosis. Hum. Gene Ther. Methods *23*, 324–335.

44. Rutledge, E.A., Halbert, C.L., and Russell, D.W. (1998). Infectious clones and vectors derived from adeno-associated virus (AAV) serotypes other than AAV type 2. J. Virol. *72*, 309–319.

45. Cearley, C.N., and Wolfe, J.H. (2007). A single injection of an adeno-associated virus vector into nuclei with divergent connections results in widespread vector distribution in the brain and global correction of a neurogenetic disease. J. Neurosci. *27*, 9928–9940.

46. Choudhury, S.R., Harris, A.F., Cabral, D.J., Keeler, A.M., Sapp, E., Ferreira, J.S., Gray-Edwards, H.L., Johnson, J.A., Johnson, A.K., Su, Q., et al. (2016). Widespread central nervous system gene transfer and silencing after systemic delivery of novel AAV-AS vector. Mol. Ther. *24*, 726–735.

47. Watson, D.J., Passini, M.A., and Wolfe, J.H. (2005). Transduction of the choroid plexus and ependyma in neonatal mouse brain by vesicular stomatitis virus glycoprotein-pseudotyped lentivirus and adeno-associated virus type 5 vectors. Hum. Gene Ther. *16*, 49–56.

48. Donsante, A., Yi, L., Zerfas, P.M., Brinster, L.R., Sullivan, P., Goldstein, D.S., Prohaska, J., Centeno, J.A., Rushing, E., and Kaler, S.G. (2011). ATP7A gene addition to the choroid plexus results in long-term rescue of the lethal copper transport defect in a Menkes disease mouse model. Mol. Ther. *19*, 2114–2123.

49. Haddad, M.R., Donsante, A., Zerfas, P., and Kaler, S.G. (2013). Fetal brain-directed AAV gene therapy results in rapid, robust, and persistent transduction of mouse choroid plexus epithelia. Mol. Ther. Nucleic Acids *2*, e101.

50. Wolfe, J.H., Kyle, J.W., Sands, M.S., Sly, W.S., Markowitz, D.G., and Parente, M.K. (1995). High level expression and export of beta-glucuronidase from murine mucopolysaccharidosis VII cells corrected by a double-copy retrovirus vector. Gene Ther. *2*, 70–78.

51. Samaranch, L., Pérez-Cañamás, A., Soto-Huelin, B., Sudhakar, V., Jurado-Arjona, J., Hadaczek, P., Ávila, J., Bringas, J.R., Casas, J., Chen, H., et al. (2019). Adeno-associated viral vector serotype 9-based gene therapy for niemann-pick disease type A. Sci. Transl. Med. *11*, eaat3738.

52. Taghian, T., Marosfoi, M.G., Puri, A.S., Cataltepe, O.I., King, R.M., Diffie, E.B., Maguire, A.S., Martin, D.R., Fernau, D., Batista, A.R., et al. (2020). A safe and reliable technique for CNS delivery of AAV vectors in the cisterna magna. Mol. Ther. *28*, 411–421.

53. Zingg, B., Peng, B., Huang, J., Tao, H.W., and Zhang, L.I. (2020). Synaptic specificity and application of anterograde transsynaptic AAV for probing neural circuitry. J. Neurosci. *40*, 3250–3267.

54. Iliff, J.J., Wang, M., Liao, Y., Plogg, B.A., Peng, W., Gundersen, G.A., Benveniste, H., Vates, G.E., Deane, R., Goldman, S.A., et al. (2012). A paraventricular pathway facilitates CSF flow through the brain parenchyma and the clearance of interstitial solutes, including amyloid β. Sci. Transl. Med. *4*, 147ra111.

55. Murlidharan, G., Crowther, A., Reardon, R.A., Song, J., and Asokan, A. (2016). Glymphatic fluid transport controls paravascular clearance of AAV vectors from the brain. JCI Insight *1*, e88034.

56. Katz, M.L., Tecedor, L., Chen, Y., Williamson, B.G., Lysenko, E., Wininger, F.A., Young, W.M., Johnson, G.C., Whiting, R.E.H., Coates, J.R., and Davidson, B.L. (2015). AAV gene transfer delays disease onset in a TPP1-deficient canine model of the late infantile form of Batten disease. Sci. Transl. Med. *7*, 313ra180.

57. Markakis, E.A., Vives, K.P., Bober, J., Leichtle, S., Leranth, C., Beecham, J., Elsworth, J.D., Roth, R.H., Samulski, R.J., and Redmond, D.E., Jr. (2010). Comparative transduction efficiency of AAV vector serotypes 1-6 in the substantia nigra and striatum of the primate brain. Mol. Ther. *18*, 588–593.

58. Dodiya, H.B., Bjorklund, T., Stansell, J., III, Mandel, R.J., Kirik, D., and Kordower, J.H. (2010). Differential transduction following basal ganglia administration of distinct pseudotyped AAV capsid serotypes in nonhuman primates. Mol. Ther. *18*, 579–587.

59. Di Pasquale, G., Davidson, B.L., Stein, C.S., Martins, I., Scudiero, D., Monks, A., and Chiorini, J.A. (2003). Identification of PDGFR as a receptor for AAV-5 transduction. Nat. Med. *9*, 1306–1312.

60. Pillay, S., Meyer, N.L., Puschnik, A.S., Davulcu, O., Diep, J., Ishikawa, Y., Jae, L.T., Wosen, J.E., Nagamine, C.M., Chapman, M.S., and Carette, J.E. (2016). An essential receptor for adeno-associated virus infection. Nature *530*, 108–112.

61. Pillay, S., Zou, W., Cheng, F., Puschnik, A.S., Meyer, N.L., Ganaie, S.S., Deng, X., Wosen, J.E., Davulcu, O., Yan, Z., et al. (2017). Adeno-associated virus (AAV) serotypes have distinctive interactions with domains of the cellular AAV receptor. J. Virol. *91*. e00391-17.

62. Zhang, R., Xu, G., Cao, L., Sun, Z., He, Y., Cui, M., Sun, Y., Li, S., Li, H., Qin, L., et al. (2019). Divergent engagements between adeno-associated viruses with their cellular receptor AAVR. Nat. Commun. *10*, 3760.

63. Ciesielska, A., Hadaczek, P., Mittermeyer, G., Zhou, S., Wright, J.F., Bankiewicz, K.S., and Forsayeth, J. (2013). Cerebral infusion of AAV9 vector-encoding non-self proteins can elicit cell-mediated immune responses. Mol. Ther. *21*, 158–166.

64. Samaranch, L., Sebastian, W.S., Kells, A.P., Salegio, E.A., Heller, G., Bringas, J.R., Pivirotto, P., DeArmond, S., Forsayeth, J., and Bankiewicz, K.S. (2014). AAV9-mediated expression of a non-self protein in nonhuman primate central nervous system triggers widespread neuroinflammation driven by antigen-presenting cell transduction. Mol. Ther. *22*, 329–337.

65. Yang, C., Hao, F., He, J., Lu, T., Klein, R.L., Zhao, L.-R., and Duan, W.-M. (2016). Sequential adeno-associated viral vector serotype 9-green fluorescent protein gene transfer causes massive inflammation and intense immune response in rat striatum. Hum. Gene Ther. *27*, 528–543.

66. Khabou, H., Cordeau, C., Pacot, L., Fisson, S., and Dalkara, D. (2018). Dosage thresholds and influence of transgene cassette in adeno-associated virus-related toxicity. Hum. Gene. Ther. *29*, 1235–1241.

67. Lock, M., Alvira, M.R., Chen, S.-J., and Wilson, J.M. (2014). Absolute determination of single-stranded and self-complementary adeno-associated viral vector genome titers by droplet digital PCR. Hum. Gene Ther. Methods *25*, 115–125.